An Overview and Statistical Study on Photocatalytic Activities of Fe based metal oxide Nanoparticles

Tahzib Ibrahim Protik
Nano Research Centre

Kristi Priya Choudhury
Nano Research Centre

Neogi, Newton
Nano Research Centre

Hossain, Sabbir
Nano Research Centre

他

https://doi.org/10.5109/7158005

出版情報：Proceedings of International Exchange and Innovation Conference on Engineering & Sciences (IEICES). 9, pp.384-390, 2023-10-19. 九州大学大学院総合理工学府
バージョン：

An Overview and Statistical Study on Photocatalytic Activities of Fe based metal oxide Nanoparticles

Tahzib Ibrahim Protik[1*], Kristi Priya Choudhury[1], Newton Neogi[1], Sabbir Hossain[1], Asraf Ibna Helal[1, 2], MD. Golam Sazid[1]
[1]Nano Research Centre, Bangladesh
[2]Department of Statistics, Shahjalal University of Science and Technology, Sylhet-3114, Bangladesh
*Corresponding author email: tahzib.ibrahim@gmail.com

Abstract: *Nanomaterials (NMs) are anticipated to have a significant impact on multiple sectors due to their potential to enhance performance, enhance safety, and be synthesized through novel methods. The utilization of Fe_3O_4 nanoparticles (NPs) is advantageous compared to other materials because of the diminutive size and elevated surface area to volume ratio of these NPs. The increasing significance of Fe_3O_4 NPs in environmental applications is attributed to their photocatalytic properties. The assessment of the photocatalytic efficacy of Fe_3O_4 NPs was conducted through the observation of various dyes, such as methylene blue (MB), methyl red (MR), and* Rhodamine B *(RB). Fe_3O_4 has been utilized by multiple researchers for the purpose of degrading diverse dyes. The photocatalytic efficacy of Fe_3O_4 NPs is contingent upon various factors, including their crystalline morphology, particle dimensions, and other pertinent parameters. Our research will elucidate the variables that influence the efficiency of Fe_3O_4 dye degradation.*

Keywords: NPs; Fe_3O_4 NPs, Photocatalytic activities; Dye degradation.

1. INTRODUCTION

Now a days NPs are utilized for several applications [1,2]. Photocatalysis is such an application. The process of photocatalysis, a type of catalysis, can change the rate of a photoreaction, which is a chemical reaction in which one or more reacting species absorb light. Catalysts that participate in the chemical reaction without being consumed by it are added to achieve this [3][4]. The process of "photocatalysis" uses light's energy to sequentially catalyze several chemical reactions. Every time light is absorbed by a substance, an excited electron-hole pair is produced [5] [6]. Metal oxide NPs (MONs) has been used most frequently as a photocatalyst due to its stability and low-energy band-gap. Without a shadow of a doubt, it has been demonstrated that this state-of-the-art oxidation technology is capable of destroying aquatic microorganisms [7][8]. Due to its great qualities, including excellent optical and electrical properties, high photocatalytic activity, high chemical stability, low cost, non-toxicity, and environmental friendliness, TiO_2 is a promising material that has gained widespread usage in photocatalytic processes. TiO_2 has emerged as a promising material among the other semiconductors and is frequently utilized in photocatalytic procedures [9][10]. The use of semiconductors in heterogeneous photocatalysis, on the other hand, demonstrates a significant amount of promise in terms of the reduction of these pollutants [11]. Iron oxide has become a key component in the breakdown of a variety of organic contaminants and colors due to its suitable band gap, widespread visible light harvesting, good stability, and recyclable nature. For this reason it is one of the potential photocatalysts. In addition, it has been discovered that Fe_3O_4 possesses magnetic properties, and that it is possible to recycle and reuse it by the application of an external magnetic field. This can, in the end, lead to a reduction in the costs associated with recovery treatment. Significant restrictions are placed on the use of Fe_3O_4 in the Fenton reaction for the purpose of oxidizing organic contaminants that are found in water. These limitations include the requirement that H_2O_2 be used during the reaction that was supplied from the outside, as well as the requirement that the surrounding environment be acidic in order for the Fenton reaction to produce free radicals. Fe_3O_4 provides an extra advantage due to the presence of the ions Fe^{2+} and Fe^{3+} inside its structure. These ions contribute to the continued progression of the Fenton reaction. As a consequence of this, a large number of researchers have found success in employing Fe_3O_4 as a co-catalyst within the photocatalytic system [12]. During the course of this study, data was gathered on a variety of magnetite NPs, with a particular focus on the size of these NPs as well as their effect on the deterioration of a variety of colors. A tabular record was made on the basis of the data that was obtained in order to demonstrate the time period required for the degradation of colors brought about by the magnetite NPs. We conducted statistical research to determine which magnetite NPs are most effective at degrading different colors, and based on our findings, we have concluded that smaller magnetite NPs are more successful. We were able to get a good approximation of the correlation coefficient between the dye and the effectiveness of magnetite NPs in the process of dye degradation by making use of statistical analysis. This allowed us to determine whether or not the dye was able to be degraded. The primary focus of this investigation pertains to the efficacy of Fe_3O_4 NPs in the realm of photocatalysis.

2. PHOTOCATALYTIC EFFECT OF Fe BASED NPs

Fe_3O_4 NPs are promising for RB degradation (see Fig. 1). These NPs have been examined against RB dye. 12.47 nm was the size of the particle. After 60 minutes, the degrading efficiency was 99.5% [13]. The RB dye was examined against $Fe_3O_4@SiO_2@TiO_2$. The particle has an 80 nm diameter. After 120 minutes, efficiency was 86.64% [14].The $Fe_3O_4@SiO_2@TiO_2$ NPs was applied to the RB dye. The measured particle size was 30 nanometers. After forty minutes, the rate of decay was

64% [15]. The composite Fe_3O_4-TiO_2:Eu has been examined against RB dye. Each particle measured 10.35 nm. The degradation rate was 85% after 180 minutes [16]. Once again, the RB dye was put through testing using Fe_3O_4.The average size of the particles was measured to be 9.4 nm. After an interval of 120 minutes, the level of efficiency had dropped to 56% [17]. In a different set of experiments, the RB dye was investigated with the help of Fe_3O_4-S. The particles were found to have a size of 7 nanometers when measured. After 120 minutes the degradation rate was 85.6% [17].

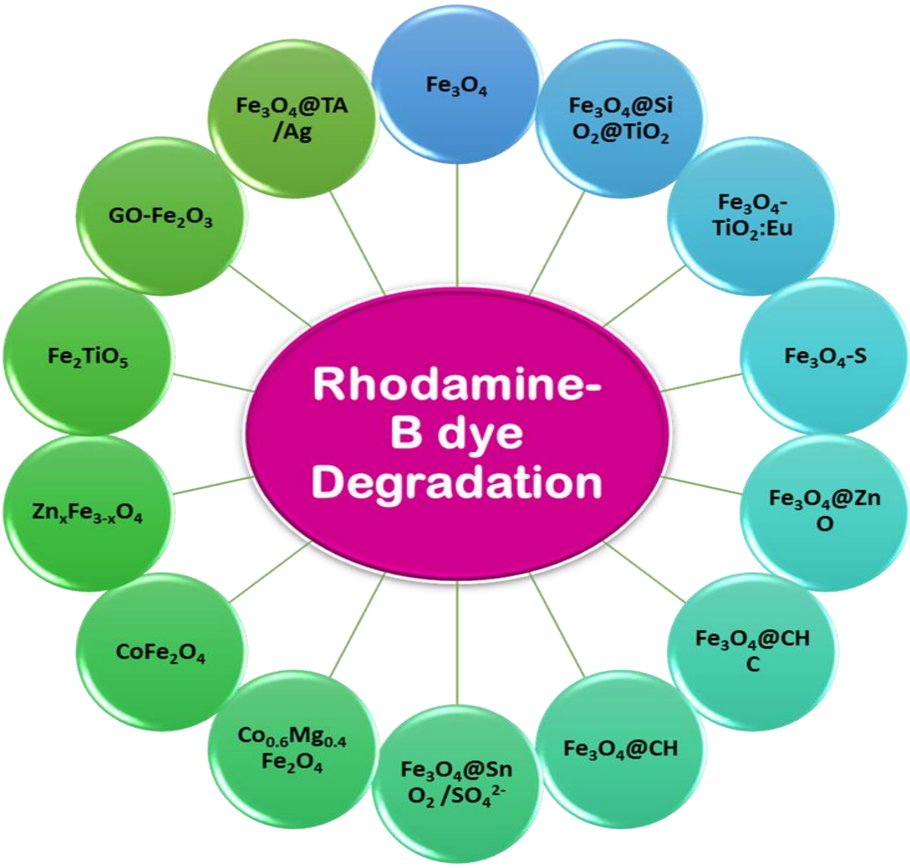

Fig. 1. RB degradation by Fe based NPs.

Testing of Fe_3O_4@ZnO NPs against RB dye has been done. The particle size was 60 nm. After 60 minutes, the degradation efficiency was 99.3% [18]. The Fe_3O_4@CHC material has been utilized in a study to assess its efficacy against RB dye. The size of the particle measured 3.054 nanometers. After a duration of 180 minutes, the efficiency of degradation was found to be 98.3% [19]. A comparative analysis has been conducted between the Fe_3O_4@CH composite and RB dye. The particle's dimensions were quantified to be 6.019 nanometers in magnitude. After a time period of 180 minutes, the degradation efficacy was observed to be 92.9% [19]. Fe_3O_4 has been utilized to test to RB dye. The sample contained particles with a size of 10.42 nanometers. After a duration of 180 minutes, the degradation efficiency was recorded to be 71.8% [19].

The efficacy of Fe_3O_4@SnO_2/SO_4^{2-} was evaluated in relation to its ability to degrade RB dye. The size of the particles was observed to fall within the range of 40 to 45 nanometers. Following a 240-minute period, the degradation efficiency was determined to be 73% [20]. The compound $Co_{0.6}Mg_{0.4}Fe_2O_4$ has been employed as a counteragent to RB dye. The measured particle size was 39 nanometers. Following a duration of 180 minutes, the degradation efficacy was determined to be 99.5 percent [21]. The utilization of $CoFe_2O_4$ has been employed for the purpose of evaluating RB dye. The dimensions of the particles measured 46 nanometers. Following a duration of 180 minutes, a proportion of 73% of the damage had been incurred [21]. Zn_xFe_{3-x} was employed for the treatment of RB dye. The particles exhibited a size distribution within the range of 10 to 12 nanometers. Following a duration of 300 minutes, the efficiency of degradation was recorded at 97.31 percent [22]. A study was conducted on the impact of Fe_2TiO_5 on RB dye. The dimensions of the particles were measured to be 20 nanometers. Following a duration of 240 minutes, the degradation process exhibited a level of efficiency amounting to 96% [23]. RB dye and GO-Fe_2O_3 were subjected to experimental evaluation. The particle size was 20 nm. The degradation efficiency was observed to be 90.9% following an 80-minute duration [24]. The utilization of Fe_3O_4@TA/Ag composite has been observed in the context of RB dye. The size distribution of the nanoparticle was observed to fall within the range of 10-15 nanometers. Following a period of 60 seconds, the degradation efficiency was noted to be 99% [25]. The composite of $CoFe_2O_4$@5ZnO has been subjected to experimentation using MB dye. The particle's dimensions were determined to be 14.9 nanometers through measurement. Following duration of 180 minutes, it was observed that the degradation rate amounted to 78.3%. The utilization of $CoFe_2O_4$@4ZnO composite material has been implemented as a strategy for alleviating the impact of MB dye. The particle dimensions were determined to be 18.1 nanometers through measurement. After a time period of 180 minutes, the rate of decomposition was observed to be 65.5%. The efficacy of MB dye has been evaluated in conjunction with $CoFe_2O_4$@3ZnO.The dimensions of the particles were measured to be 19 nanometers. Following a duration of 180 minutes, the rate of degradation amounted to 60.5% [26]. The efficacy of Fe_3O_4/acid chloride/titanium dioxide has been evaluated in the context of its application towards the removal of MB dye. The size of the particles was determined to be 18.3 nm. Following a duration of 60 minutes, the degradation efficacy exhibited a rate of 98 percent[27]. A study was conducted on the impact of Fe_2O_3/TiO_2 on the degradation of MB dye. The size of the particles was measured to be 7 nanometers. Following a duration of sixty minutes, the level of deterioration had attained a magnitude of 30 percent [28]. The Fe_3O_4/TiO_2/CuO composite has been utilized in the degradation of MB dye. The size of the particle was measured to be 8 nanometers. After a duration of 22 minutes, the efficiency of degradation was observed to be 99.78% [29]. The efficacy of the MB dye has been evaluated through experimentation involving $BiVO_4/Fe_3O_4/C_{60}$. The particle size was 14.89 nm. Following a duration of 300 minutes, the deterioration efficiency was observed to be 64% [30]. The effectiveness of the Fe_3O_4@TiO_2/Ag, Cu composite in mitigating the impact of MB dye has been investigated. The particle's dimensions fell within the range of 40-50 nanometers. Following a time period of 90 minutes, the degradation efficiency was determined to be 86.19% [31]. An experiment was conducted utilizing Fe_3O_4@TA/Ag to assess the efficacy of MB dye. The study employed a particle size range of 10-15 nm. After a duration of 0.67 minutes, a significant proportion of 99% of the degradation process was deemed to be effective [25]. The efficacy of SnO_2@Fe_3O_4 nanocomposite in mitigating the impact of MB dye has been exhibited. The size of the particles varied between 25 and 35 nanometers. Following duration of 120 minutes, the degradation efficiency was recorded at 88.3 percent [32]. The efficacy of Fe_3O_4 NPs has been evaluated in relation to their ability to mitigate the effects of MB dye. The measured particle size was 30 nanometers. After duration of 180 minutes, 60% of the degradation efficiency was observed [33]. The utilization of MB dye has been employed in the examination of MB dye. Each particle exhibited a size of 40 nanometers. Following a duration of 240 minutes, the rate of degradation amounted to 86.58% [34]. The MB dye underwent treatment utilizing EDTA@Fe_3O_4/SC. Particles ranging from 10 to 20 nanometers in size were observed. Following a duration of 90 minutes, the efficiency of degradation had attained a level of 99.5% [35]. The present study employed MgAC-Fe_3O_4/TiO_2 as the test material to evaluate its efficacy against MB dye. The dimensions of the particles were ascertained to be 32.82 nanometers. Following a duration of twenty minutes, the degradation process exhibited a level of efficiency amounting to 93% [36]. The efficacy of Fe_3O_4 has been evaluated in relation to its interaction with MB dye. The particle size was 7.8 nm. The degradation efficiency reached 89% within duration of 140 minutes. The efficacy of Fe_3O_4@TiO_2 composite against MB dye has been investigated through experimentation. The particle's dimensions were determined to be 73 nanometers. After a time period of 140 minutes, the effectiveness of degradation observed was 56% [37]. Experiments have been carried out utilizing (Cu/Ni)-Al layered double hydroxides@Fe_3O_4 for the purpose of conducting anti-MB dye studies. The particles exhibited a size distribution within the range of 4 to 10 nanometers. Following duration of 90 minutes, the rate of degradation exhibited an optimal level of 100% [38]. The effectiveness of Fe_3O_4 NPs has been assessed in the context of ameliorating the impact of MB dye. The dimensions of the particle were determined to be 20.7 nanometers. Following a time span of 180 minutes, the degradation efficiency was determined to be 71% [39]. Fe_3O_4 NPs were utilized in experiments conducted with MB dye. The particles measured 30 nanometers in size. After duration of 120 minutes, the degradation efficiency was recorded to be 71.36% [40]. The efficacy of the $Ag_3PO_4/Fe_3O_4/C_{60}$ composite was evaluated in the context of its application towards the degradation of MB dye. The size of the particle was measured to be 31.75 nanometers. Following duration of 300 minutes, the rate of deterioration had achieved a level of 95% efficiency [40]. Moreover, Fe_3O_4 NPs showed 100% efficiency with respect to MR after 360 min [41]. Fe_3O_4@SiO_2@NH_2 demonstrate degradation efficiency of 84.9% after 120 with MR [42]. Fe_3O_4-Fe_2O_2@SiO_2 composite showed an efficiency of 98% after 180 min with same dye (see Fig. 2) [43].

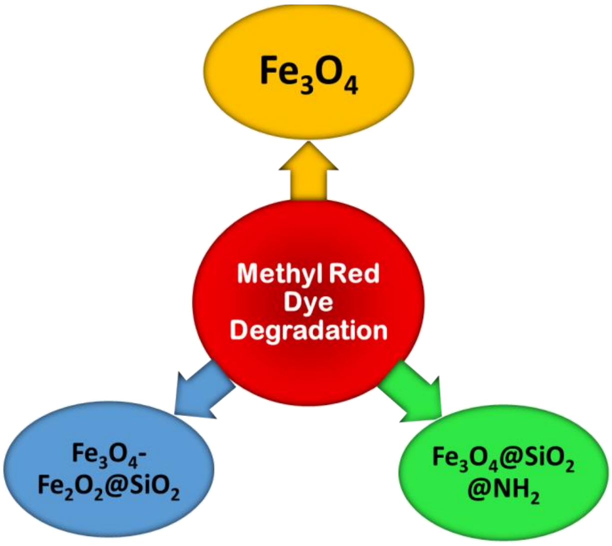

Fig. 2. MR degradation by Fe based NPs.

3. METHODOLOGY

We have 40 data of Fe_3O_4 NPs for data analysis. There 3 variables of the data such as, Size, Efficiency, Dye name and Duration of work of Fe_3O_4 NPs. There, we perform descriptive analysis and correlation to make our result more precise and to find factor affecting the efficiency of NPs. We use SPSS-version 25 for the data analysis. We make the variables categorical for convenience of the data analysis. We make the variables categorical for convenience of the data analysis.

Table 1: Table of categorical variables introduction

Name of Variables	Category	Description
NPs Efficiency	Most Efficient	Equal & above 80%

	Efficient	Below 80%
NPs Size	1 is (<30)	Size is less than 30 nm
	2 is (>=30)	Size is equal and above 30
Name of Dye	1	RB
	2	MB
	3	Methyl Red

4. TABLE OF THE COLLECTED DATA

Table 2: Fe3O4 NPs with different dye

NP name	Size (nm)	Dye	Efficiency (%)	Time (min)	Ref.
Fe_3O_4	12.47	RB	99.50	60	[13]
$Fe_3O_4@SiO_2@TiO_2$	80	RB	86.64	120	[14]
$Fe_3O_4@SiO_2@TiO_2$	30	RB	64	40	[15]
Fe_3O_4-TiO_2:Eu	10.35	RB	85	180	[16]
Fe_3O_4	9.4	RB	56	120	[17]
Fe_3O_4-S	7	RB	85.60	120	[17]
$Fe_3O_4@ZnO$	60	RB	99.30	60	[18]
Fe_3O_4@CHC	3.054	RB	98.30	180	[19]
Fe_3O_4@CH	6.019	RB	92.90	180	[19]
Fe_3O_4	10.42	RB	71.80	180	[19]
$Fe_3O_4@SnO_2/SO_4^{2-}$	40-45	RB	73	240	[20]
$Co_{0.6}Mg_{0.4}Fe_2O_4$	39	RB	99.50	180	[21]
$CoFe_2O_4$	46	RB	73.00	180	[21]
$Zn_xFe_{3-x}O_4$	10-12	RB	97.31	300	[22]
Fe_2TiO_5	20	RB	96	240	[23]
GO-Fe_2O_3	20	RB	90.90	80	[24]
Fe_3O_4@TA/Ag	10-15	RB	99	60	[25]
$CoFe_2O_4$@5ZnO	14.9	MB	78.30	180	[26]
$CoFe_2O_4$@4ZnO	18.1	MB	65.50	180	[26]
$CoFe_2O_4$@3ZnO	19	MB	60.50	180	[26]
Fe_3O_4/AC/TiO_2	18.3	MB	98	60	[27]
Fe_2O_3/TiO_2	7	MB	30	60	[28]
$Fe_3O_4/TiO_2/CuO$	8	MB	99.78	22	[29]
$BiVO_4/Fe_3O_4/C_{60}$	14.89	MB	64	300	[30]
$Fe_3O_4@TiO_2$/Ag,Cu	40-50	MB	86.19	90	[31]
Fe_3O_4@TA/Ag	10-15	MB	99	40	[25]
$SnO_2@Fe_3O_4$	25-35	MB	88.30	120	[32]
Fe_3O_4 NPs	30	MB	60	180	[33]
Ce/MTiO_2/Fe_3O_4	40	MB	86.58	240	[34]
EDTA@Fe_3O_4/SC	10-20	MB	99.50	90	[35]
MgAC-Fe_3O_4/TiO_2	32.82	MB	93	20	[36]
Fe_3O_4	7.8	MB	89	140	[37]
$Fe_3O_4@TiO_2$	73	MB	56	140	[37]
(Cu/Ni)–Al hydroxides@Fe_3O_4	4-10	MB	100	90	[38]
Fe_3O_4 NPs	20.7	MB	71	180	[39]
Fe_3O_4 NPs	30	MB	71.36	120	[40]
$Ag_3PO_4/Fe_3O_4/C_{60}$	31.75	MB	95	300	[40]
Fe_3O_4	10	MR	100	360	[41]
$Fe_3O_4@SiO_2@NH_2$	13	MR	84.9	120	[42]
Fe_3O_4-$Fe_2O_2@SiO_2$	10–12	MR	98	180	[43]

5. Result and Discussion

Our descriptive analysis result is as follows,

Table 3: Frequency Distribution of TiO2 NPs

Variables	Category	Frequency	Percentages
Size	Below 30	27	67.5
	Equal & above 30	13	32.5
Dye Name	RB	17	42.5
	MB	20	50
	Methyl Red	20	7.5
Efficiency	Most Efficient	14	35
	Efficient	26	65

Table 3 presents the frequency distribution of Fe_3O_4 NPs. The data exhibits a distinct demarcation, with 67.5% of the observations falling below the 30 nm threshold and the remaining observations distributed equally or above this threshold. The data indicates that the dye degradation activities for RB , MB , and methyl red dye are 42.5%, 50%, and 7.5%, respectively. The Fe_3O_4 NPs exhibit an efficiency of 35% in terms of degradation, while the remaining 65% of the NPs demonstrate efficacy in dye degradation.

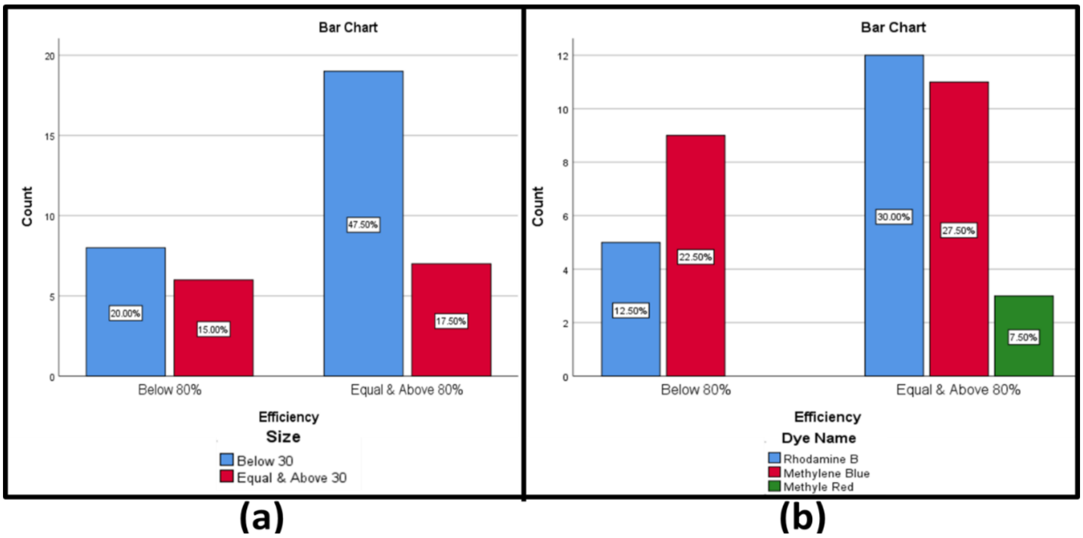

Fig. 3. (a) Size vs Efficiency Bar Chart (b) Dye vs Efficiency Bar Chart

The data indicates that 47.5% of NPs with the highest level of efficiency possess sizes that fall below 30, while 17.5% exhibit sizes that are equal to or greater than 30. In contrast, it can be observed that 20% of Fe_3O_4 NPs exhibit high efficiency with sizes below 30, while 15% of the NPs demonstrate sizes equal to or exceeding 30 (see Fig. 3(a)).

According to the data presented in Figure 3(b), it can be observed that 30% of the Fe_3O_4 NPs with the highest level of efficiency exhibit degradation of RB dye, thereby demonstrating their efficacy. Conversely, 12.5% of the efficient NPs demonstrate their effectiveness by means of RB dye degradation. The percentages of highly efficient NPs and NPs that exhibit efficiency in the degradation of MB dye are 27.5% and 22.5%, respectively. According to our data, the proportion of highly effective NPs and the frequency of effective NPs in the process of methyl red degradation are 7.5% and 0%, respectively (see Fig. 3(b)).

Now the result of the bivariate correlation is as follows:

Table 4: Bivariate Correlation Result

		Sizes of NPs	Dye Name	Efficiency
Size of NPs	Pearson Correlation	1	-.126	-.126
Dye Name	Pearson Correlation	-.126	1	0.009
Efficiency	Pearson Correlation	-.126	.009	1

Table 4 displays the correlation between efficiency and the two additional variables, namely size and dye name. The data indicates that there exists a negative correlation of -0.126 between the variables of size and efficiency. This implies the presence of a negative correlation between size and efficiency over a period of one week. This implies that an increase in size will result in a reduction in the efficacy of photocatalysis. A decrease in size is expected to result in an increase in efficiency. Furthermore, it is observed that the correlation coefficient between dye and efficiency is 0.009. This implies a tenuous correlation between dye and efficacy.

The findings suggest that the degradation of various dyes remains consistent for Fe_3O_4 NPs.

6. CONCLUSION

The conclusion section presents a comprehensive portrayal of Fe_3O_4 NPs through a descriptive analysis. The degradation of dye by NPs was observed in relation to both the size of the NPs and the type of dye utilized. A correlation analysis revealed a negative and statistically significant association between size and efficiency. This study found inverse relationship between the rate of dye degradation and the size of NPs. Furthermore, a tenuous correlation was observed between the dye and the efficacy of Fe_3O_4 NPs. It can be inferred that an inverse relationship exists between the size and efficiency of photocatalysis, whereby an increase in size results in a decrease in efficiency. A decrease in size is expected to result in an increase in efficiency. So, we can say that the efficacy of dye degradation with photocatalysis depends on the particle size.

7. REFERENCES

[1] A. Kalbekov, E. Omurzak, Properties of ZnO and Zn Nanoparticles Produced by Electrical Discharge in Liquid Method, Proceedings of International Exchange and Innovation Conference on Engineering & Sciences (IEICES), 8 (2022) 335–339.

[2] Islam M. Radwan, O. Eljamal, A mini-Review on Transportation and Fate of Silver Nanoparticles Released from Consumer Products: Ecological Risk Assessments, Proceedings of International Exchange and Innovation Conference on Engineering & Sciences (IEICES), 8 (2022) 52–61.

[3] D. Beydoun, R. Amal, G. Low, S. McEvoy, Role of nanoparticles in photocatalysis, Journal of Nanoparticle Research, 1 (1999) 439–458.

[4] L. Liu, X. Zhang, L. Yang, L. Ren, D. Wang, J. Ye, Metal nanoparticles induced photocatalysis, Natl Sci Rev, 4 (2017) 761–780.

[5] A. Gellé, A. Moores, Plasmonic nanoparticles: Photocatalysts with a bright future, Curr Opin Green Sustain Chem, 15 (2019) 60–66.

[6] A.A. Ansari, M. Sillanpää, Advancement in upconversion nanoparticles based NIR-driven

photocatalysts, Renewable and Sustainable Energy Reviews, 151 (2021) 111631.
[7] S.M. Gupta, M. Tripathi, An overview of commonly used semiconductor nanoparticles in photocatalysis, High Energy Chemistry, 46 (2011) 1–9.
[8] U. Qumar, J.Z. Hassan, R.A. Bhatti, A. Raza, G. Nazir, W. Nabgan, M. Ikram, Photocatalysis vs adsorption by metal oxide nanoparticles, J Mater Sci Technol, 131 (2022) 122–166.
[9] D. Beydoun, R. Amal, G. Low, S. McEvoy, Role of nanoparticles in photocatalysis, Journal of Nanoparticle Research, 1 (1999) 439–458.
[10] M. Sagir, M.B. Tahir, J. Akram, M.S. Tahir, U. Waheed, Nanoparticles and Significance of Photocatalytic Nanoparticles in Wastewater Treatment: A Review, Curr Anal Chem, 17 (2020) 38–48.
[11] M. Mousavi, A. Habibi-Yangjeh, D. Seifzadeh, K. Nakata, S. Vadivel, Exceptional photocatalytic activity for g-C_3N_4 activated by H_2O_2 and integrated with Bi_2S_3 and Fe_3O_4 nanoparticles for removal of organic and inorganic pollutants, Advanced Powder Technology, 30 (2019) 524–537.
[12] C. Shan, Z. Su, Z. Liu, R. Xu, J. Wen, G. Hu, T. Tang, Z. Fang, L. Jiang, M. Li, One-Step Synthesis of Ag2O/Fe3O4 Magnetic Photocatalyst for Efficient Organic Pollutant Removal via Wide-Spectral-Response Photocatalysis–Fenton Coupling, Molecules, 28 (2023) 4155.
[13] A. Radoń, S. Łoński, T. Warski, R. Babilas, T. Tański, M. Dudziak, D. Łukowiec, Catalytic activity of non-spherical shaped magnetite nanoparticles in degradation of Sudan I, Rhodamine B and Methylene Blue dyes, Appl Surf Sci, 487 (2019) 1018–1025.
[14] F. Chen, F. Yan, Q. Chen, Y. Wang, L. Han, Z. Chen, S. Fang, Fabrication of Fe_3O_4@SiO_2@TiO_2 nanoparticles supported by graphene oxide sheets for the repeated adsorption and photocatalytic degradation of rhodamine B under UV irradiation, Dalton Transactions, 43 (2014) 13537–13544.
[15] M.P. Mazhari, A. Abbasi, A. Derakhshan, M. Ahmadi, Fabrication $Fe_3O_4/SiO_2/TiO_2$ Nanocomposites and Degradation of Rhodamine B Dyes under UV Light Irradiation, J. Nanostruct, 6 (2016) 101–105.
[16] M. Stefan, C. Leostean, O. Pana, D. Toloman, A. Popa, I. Perhaita, M. Senilă, O. Marincas, L. Barbu-Tudoran, Magnetic recoverable Fe_3O_4-TiO_2:Eu composite nanoparticles with enhanced photocatalytic activity, Appl Surf Sci, 390 (2016) 248–259.
[17] B. Caglar, E.K. Guner, K. Keles, K.V. Özdokur, O. Cubuk, F. Coldur, S. Caglar, C. Topcu, A. Tabak, Fe_3O_4 nanoparticles decorated smectite nanocomposite: Characterization, photocatalytic and electrocatalytic activities, Solid State Sci, 83 (2018) 122–136.
[18] J. Wang, J. Yang, X. Li, D. Wang, B. Wei, H. Song, X. Li, S. Fu, Preparation and photocatalytic properties of magnetically reusable Fe_3O_4@ZnO core/shell nanoparticles, Physica E Low Dimens Syst Nanostruct, 75 (2016) 66–71.
[19] X. Zhu, L. Zhang, G. Zou, Q. Chen, Y. Guo, S. Liang, L. Hu, M. North, H. Xie, Carboxylcellulose hydrogel confined-Fe_3O_4 nanoparticles catalyst for Fenton-like degradation of Rhodamine B, Int J Biol Macromol, 180 (2021) 792–803.
[20] H. Ghafuri, F. Mohammadi, R. Rahimi, E. Mohammadiyan, Synthesis and characterization of a new magnetic nanocomposite with metalloporphyrin (Co-TPyP) and sulfated tin dioxide (Fe_3O_4@SnO_2/SO_4^{2-}), and investigation of its photocatalytic effects in the degradation of Rhodamine B, RSC Adv, 6 (2016) 83947–83953.
[21] M. Sundararajan, L. John Kennedy, P. Nithya, J. Judith Vijaya, M. Bououdina, Visible light driven photocatalytic degradation of rhodamine B using Mg doped cobalt ferrite spinel nanoparticles synthesized by microwave combustion method, Journal of Physics and Chemistry of Solids, 108 (2017) 61–75.
[22] A. Manohar, K. Chintagumpala, K.H. Kim, Magnetic hyperthermia and photocatalytic degradation of rhodamine B dye using Zn-doped spinel Fe_3O_4 nanoparticles, Journal of Materials Science: Materials in Electronics, 32 (2021) 8778–8787.
[23] S. Zhang, P. Shen, M. Ge, X. Zhu, N. Ali, L. Ni, Fabricating Fe2TiO5 hollow microspheres with enhanced visible light photocatalytic activity, Mater Res Express, 6 (2019) 095505.
[24] S. Guo, G. Zhang, Y. Guo, J.C. Yu, Graphene oxide–Fe2O3 hybrid material as highly efficient heterogeneous catalyst for degradation of organic contaminants, Carbon N Y, 60 (2013) 437–444.
[25] H. Veisi, S.B. Moradi, A. Saljooqi, P. Safarimehr, Silver nanoparticle-decorated on tannic acid-modified magnetite nanoparticles (Fe_3O_4@TA/Ag) for highly active catalytic reduction of 4-nitrophenol, Rhodamine B and Methylene blue, Materials Science and Engineering: C, 100 (2019) 445–452.
[26] E. Suharyadi, A. Muzakki, A. Nofrianti, N.I. Istiqomah, T. Kato, S. Iwata, Photocatalytic activity of magnetic core-shell $CoFe_2O_4$@ZnO nanoparticles for purification of methylene blue, Mater Res Express, 7 (2020) 085013.
[27] S. Moosavi, R.Y.M. Li, C.W. Lai, Y. Yusof, S. Gan, O. Akbarzadeh, Z.Z. Chowhury, X.G. Yue, M.R. Johan, Methylene Blue Dye Photocatalytic Degradation over Synthesised $Fe_3O_4/AC/TiO_2$ Nano-Catalyst: Degradation and Reusability Studies, Nanomaterials, 10 (2020) 2360.
[28] M.A. Ahmed, E.E. El-Katori, Z.H. Gharni, Photocatalytic degradation of methylene blue dye using Fe_2O_3/TiO_2 nanoparticles prepared by sol–gel method, J Alloys Compd, 553 (2013) 19–29.
[29] A.H. Kianfar, M.A. Arayesh, Synthesis, characterization and investigation of photocatalytic and catalytic applications of Fe_3O_4/TiO_2/CuO nanoparticles for degradation of MB and reduction of nitrophenols, J Environ Chem Eng, 8 (2020) 103640.
[30] S. Sepahvand, S. Farhadi, Preparation and characterization of fullerene (C60)-modified $BiVO_4/Fe_3O_4$ nanocomposite by hydrothermal

method and study of its visible light photocatalytic and catalytic activity, 26 (2018) 417–432.
[31] H. Ghafuri, M. Dehghani, A. Rashidizadeh, M. Rabbani, Synthesis and characterization of magnetic nanocomposite Fe_3O_4@TiO_2/Ag,Cu and investigation of photocatalytic activity by degradation of rhodamine B (RhB) under visible light irradiation, Optik (Stuttg), 179 (2019) 646–653.
[32] G.G. Hasan, H.A. Mohammed, M. Althamthami, A. Khelef, S.E. Laouini, S. Meneceur, Synergistic effect of novel biosynthesis SnO_2@Fe_3O_4 nanocomposite: A comprehensive study of its photocatalytic of Dyes & antibiotics, antibacterial, and antimutagenic activities, J Photochem Photobiol A Chem, 443 (2023) 114874.
[33] B.-Y.; Wang, S.-Y.; Huang, Y.-S.; Hsiao, P.-C.; Wei, C.-M.; Chou, B.-Y. Wang, S.-Y. Huang, Y.-S. Hsiao, P.-C. Wei, C.-M. Chou, V.K.S. Hsiao, Pulsed-Laser Induced Photolysis of Synthesizing Magnetic Fe_3O_4 Nanoparticles for Visible-Light Photocatalysis, Catalysts, 12 (2022) 1459.
[34] Z. Shi, X. Yang, S. Yao, Photocatalytic activity of cerium-doped mesoporous TiO2 coated Fe3O4 magnetic composite under UV and visible light, Journal of Rare Earths, 30 (2012) 355–360.
[35] N. Kataria, V.K. Garg, Application of EDTA modified Fe_3O_4/sawdust carbon nanocomposites to ameliorate methylene blue and brilliant green dye laden water, Environ Res, 172 (2019) 43–54.
[36] V.K.H. Bui, D. Park, T.N. Pham, Y. An, J.S. Choi, H.U. Lee, O.H. Kwon, J.Y. Moon, K.T. Kim, Y.C. Lee, Synthesis of MgAC-Fe_3O_4/TiO_2 hybrid nanocomposites via sol-gel chemistry for water treatment by photo-Fenton and photocatalytic reactions, Scientific Reports, 9 (2019) 1–11.
[37] S. Dagher, A. Soliman, A. Ziout, N. Tit, A. Hilal-Alnaqbi, S. Khashan, F. Alnaimat, J.A. Qudeiri, Photocatalytic removal of methylene blue using titania- and silica-coated magnetic nanoparticles, Mater Res Express, 5 (2018) 065518.
[38] H.R. Mardani, (Cu/Ni)–Al layered double hydroxides@Fe_3O_4 as efficient magnetic nanocomposite photocatalyst for visible-light degradation of methylene blue, Research on Chemical Intermediates, 43 (2017) 5795–5810.
[39] A. V. Ramesh, D. Rama Devi, S. Mohan Botsa, K. Basavaiah, Facile green synthesis of Fe3O4 nanoparticles using aqueous leaf extract of Zanthoxylum armatum DC for efficient adsorption of methylene blue, 6 (2018) 145–155.
[40] R.N. Mogomotsi, S.S. Akinola, E.E. Emeka, O.E. Fayemi, Cyclic voltammetry, photocatalytic and antimicrobial comparative studies of fabrication Fe_3O_4 and Fe_3O_4/PAN nanofibers, Mater Res Express, 7 (2020) 055001.
[41] S.C.D. Sharma, Q. Sun, J. Li, Y. Wang, F. Suanon, J. Yang, C.P. Yu, Decolorization of azo dye methyl red by suspended and co-immobilized bacterial cells with mediators anthraquinone-2,6-disulfonate and Fe_3O_4 nanoparticles, Int Biodeterior Biodegradation, 112 (2016) 88–97.
[42] F. Ghorbani, S. Kamari, Core–shell magnetic nanocomposite of Fe_3O_4@SiO_2@NH_2 as an efficient and highly recyclable adsorbent of methyl red dye from aqueous environments, Environ Technol Innov, 14 (2019) 100333.
[43] M. Hanif Irfan, H. Sanjaya, S. Aini, Degradation of Methyl Red Using a Mixture of Iron Oxide In Silica Mesoporous, International Journal of Scientific Research and Engineering Development, 2 (2019) 597-600.